



ELSEVIER

SCIENCE @ DIRECT®

PHYSICS LETTERS B

Physics Letters B 551 (2003) 317–323

www.elsevier.com/locate/npe

Real and virtual Compton scattering in a Regge approach

F. Cano, J.-M. Laget *

CEA-Saclay, DAPNIA/SPhN, F-91191 Gif-sur-Yvette cedex, France

Received 1 October 2002; received in revised form 18 November 2002; accepted 21 November 2002

Editor: P.V. Landshoff

Abstract

We study real and deeply virtual Compton scattering in a model based on Regge trajectories and two-gluon exchange. In the kinematic regime of current experiments, the hadronic component of the outgoing real photon plays a major role. We analyze the spin structure of Compton scattering at large momentum transfer and give predictions for several spin asymmetries. In the DVCS channel, a fairly good agreement is obtained for the recently measured beam spin and charge asymmetries.

© 2002 Elsevier Science B.V. Open access under [CC BY license](http://creativecommons.org/licenses/by/4.0/).

1. Introduction

Exclusive real and virtual Compton scattering are the cleanest channels for the investigation of the structure of hadronic matter. They involve two electromagnetic couplings and leads to more complete information than other processes like deep inelastic scattering or elastic form factors.

It was recently established that, for high virtuality Q^2 , the amplitude of deeply virtual Compton scattering (DVCS) can be factorized in a hard part, which can be calculated in pQCD, and a soft universal non-perturbative part which is parameterized in terms of Generalized Parton Distributions (GPDs) (for a recent review see [1] and references therein). The existence of a hard scale (Q^2) leads to the dominance of the handbag-type diagrams, where the two photons have a

pointlike coupling with the quarks of the target. Since DVCS is a process of order α_{em}^3 , cross sections are very small and its experimental determination is a very difficult task. So far, absolute cross sections have been released only by HERA in the small x_{Bj} region [2]. The beam spin asymmetry is more accessible and has already been measured at JLab [3] and HERMES [4]. The size of this asymmetry is an indirect determination of the GPDs (more precisely, the imaginary part of the VCS amplitude). Theoretical expectations based on current modelisations of GPDs are compatible with both HERMES and JLab data but the general trend is an overestimate of the experimental points.

However, in such a range of low momentum transfer the coupling of the point like component of the final real photon might not be dominant: the contribution due to its hadronic component is not negligible. Indeed, the coherence length, or lifetime of the hadronic component, of a real photon of, let say, 4 GeV is of the order of 3 fm, larger than the size of the nucleon. This conjecture has been verified by measurements at Cornell [5] and more recently by

* Corresponding author.

E-mail addresses: fcano@cea.fr (F. Cano), jlaget@cea.fr (J.-M. Laget).

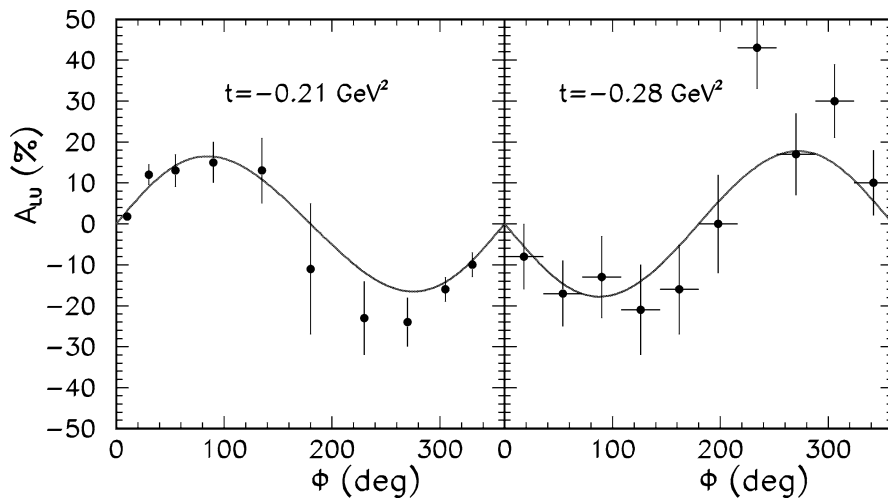


Fig. 1. Azimuthal dependence of the beam-spin asymmetries in DVCS. Data taken from CLAS [3] (left, $x_{Bj} = 0.19$, $Q^2 = 1.25 \text{ GeV}^2$, $E_{e^-} = 4.25 \text{ GeV}$) and HERMES [4] (right, $x_{Bj} = 0.11$, $Q^2 = 2.6 \text{ GeV}^2$, $E_{e^+} = 27.6 \text{ GeV}$).

HERMES [6]. The emission of the real photon occurs through the formation of a vector meson intermediate state. The photon production amplitude can simply be obtained from the vector meson production amplitude¹ just by multiplying it by the corresponding coupling constant $\sqrt{4\pi\alpha_{em}}/f_V$, where f_V is the radiative decay constant of the vector meson [7] (see also [8]). We already showed [7] that this is supported by available data on cross sections of ρ -photoproduction [9] and wide angle Compton scattering (WACS) at $E_\gamma = 4 \text{ GeV}$ [10].

In this Letter, we extend to spin observables the predictions of this effective model based on the interaction of the hadronic component of the photon with the proton through the exchange of mesons (Regge trajectories) and of two non-perturbative gluons. It turns out, Fig. 1, that it reproduces fairly well the beam spin asymmetries A_{LU} observed in DVCS, not only their $\sin\phi$ dependence, which is just a consequence of the dominance of the helicity conserving amplitude for absorbing a transverse virtual photon [11], but also their magnitude. In the kinematical range accessible by the present generation of experimental facilities, we

have not yet reached the asymptotic regime where the point like coupling of the photon dominates.

2. The theoretical framework

Let us briefly recall the main ingredients of the model for vector meson production. At high energies the interaction of the photon with the proton occurs through the exchange of Regge trajectories, which represent an economical way to take into account meson (or $q\bar{q}$) exchange. In addition, gluon exchange is also allowed and adds up to the Regge (or quark) exchange. We refer to [12] for the expression of the various gluon, meson and baryon exchange amplitudes. We give only the expression of the σ meson exchange gauge invariant amplitude, which was not given there. For ρ production, it is much larger than π exchange, and its vector part takes the form [13]:

$$\begin{aligned} \vec{J} \cdot \vec{\epsilon}_\gamma &= ie \frac{g_{\rho\sigma\gamma}}{m_\rho} g_{NN\sigma} \bar{u}(\vec{p}', s') u(\vec{p}, s) \mathcal{P}_\sigma \\ &\times [q(p - p') \vec{\epsilon}_\rho^* \cdot \vec{\epsilon}_\gamma - q \epsilon_\rho^*(\vec{p} - \vec{p}') \cdot \vec{\epsilon}_\gamma], \end{aligned} \quad (1)$$

where q refers to the momentum of the incoming photon, p and p' to the momenta of the initial and final proton. Contrary to Ref. [13] we use the Regge

¹ The photoproduction of an isovector state dominates over the isoscalar channel, so that we can keep only the ρ channel and neglect the ω channel.

propagator \mathcal{P}_σ whose expression is [14]:

$$\mathcal{P}_\sigma = \left(\frac{s}{s_0}\right)^{\alpha_\sigma(t)} \frac{\pi\alpha'_\sigma}{\Gamma(1+\alpha_\sigma(t))} \frac{e^{-i\pi\alpha_\sigma(t)}}{\sin(\pi\alpha_\sigma(t))}. \quad (2)$$

The reference scale s_0 is chosen to be 1 GeV² and the Regge trajectory is $\alpha_\sigma(t) = \alpha_\sigma^0 + \alpha'_\sigma t$ with a slope $\alpha'_\sigma = 0.7$ GeV⁻² and an intercept given by $\alpha_\sigma^0 = -\alpha'_\sigma m_\sigma^2 = -0.175$. The coupling constants are $g_{\rho\sigma\gamma} = 1$ and $g_{NN\sigma}^2/4\pi = 15$. They fall in the range of values which can be deduced from the analysis of the radiative decay width $\rho \rightarrow \gamma(\pi\pi)_S$ [15] and of nucleon–nucleon scattering [16]. Since the σ meson is a representation of the two pion S -wave continuum, there is an inherent uncertainty in their definition, and their product has been determined by fitting [12] the low energy ρ photoproduction data. As usual, an hadronic form factor, $F_\sigma(t) = \left(\frac{\Lambda^2 - m_\sigma^2}{\Lambda^2 - t}\right)^4$ with $\Lambda = 2$ GeV, is used at the $NN\sigma$ vertex. In addition, at low momentum transfer and moderate energies, also the f_2 meson exchange is important.

At large momentum transfer Regge trajectories saturate and become t independent. Saturating trajectories [14] represent an effective way to take into account the formation of a meson through the exchange of a hard gluon, and the model agrees remarkably well with data [9], in the region around 90 degrees. Finally, as the kinematical boundary in t is reached, the u -channel exchange of N and Δ becomes the dominant mechanism. A more quantitative analysis of the relative weight of each contribution in different kinematical regimes can be found in [12].

3. Real Compton scattering

In Ref. [7] we have shown how the various meson photoproduction channels at large momentum transfer single out and calibrate the various ingredients of this model. When scaled by the factor $\sqrt{4\pi\alpha_{em}}/f_V$ the ρ -photoproduction amplitudes² lead to a “parameter free” prediction of the Compton scattering amplitudes, giving access not only to the cross sections [17] but also to the various spin observables.

For instance, the energy dependence at fixed angle for $\gamma p \rightarrow p\rho$ at 90° is compatible with a s^{-7} behav-

our. The $\gamma p \rightarrow p\gamma$ cross section also follows this behaviour because the $\rho\gamma$ coupling does not introduce any extra power in s . Cornell data [10] at fixed angle were fitted to a power s^n , with $n = 7.1 \pm 0.4$ at 90°. Models based on soft overlap [18] also predict an approximate s^{-7} behavior at these angles. This is at variance with the pQCD counting rules which lead to a s^{-6} power-law. Nonetheless, more precise data is needed in order to settle with greater accuracy the energy dependence.

Polarization observables impose further constraints. Of particular interest are the asymmetries which are being measured at JLab. The longitudinal polarization transfer is defined as

$$A_{LL} \frac{d\sigma}{dt} = \frac{d\sigma(\uparrow\uparrow)}{dt} - \frac{d\sigma(\uparrow\downarrow)}{dt}, \quad (3)$$

where the first arrow indicates the (positive) polarization of the incident photon and the second one refers to the helicity of the recoiling proton.

In analogous way, we can define the transverse polarization transfer of the outgoing proton A_{LT} as:³

$$A_{LT} \frac{d\sigma}{dt} = \frac{d\sigma(\uparrow\rightarrow)}{dt} - \frac{d\sigma(\uparrow\leftarrow)}{dt}, \quad (4)$$

and the induced polarization in the normal plane P_N for unpolarized photons.

In Fig. 2 we present our results for these three polarization transfers. Our predictions are quite close the ones provided by the soft overlap mechanism [20,21] and have opposite sign with respect to the pQCD one [22]. Preliminary data from JLab [23] ($A_{LL} \approx 70\%$ at 120°) confirm our conjecture and rule out the pure asymptotic hard scattering approach. Our curve lies slightly below this experimental point.

For A_{LT} our predictions are also similar to the ones of the soft overlap approach, both in sign and in magnitude. Our prediction for the induced normal polarization is rather small, $P_N \simeq 20\%$ at most, as in the handbag approach where it is a NLO effect (order α_s).

We can trace back the origin of these asymmetries by writing the polarization transfer in a given direction

³ Following [19,20], the direction of the normal (to the scattering plane) polarization is defined as $\vec{N} = \hat{q} \times \hat{p}'$ and the transverse polarization as $\vec{T} = \vec{N} \times \hat{p}'$, the \hat{z} -direction taken along the incoming photon.

² We have retained only the transverse ρ polarization.

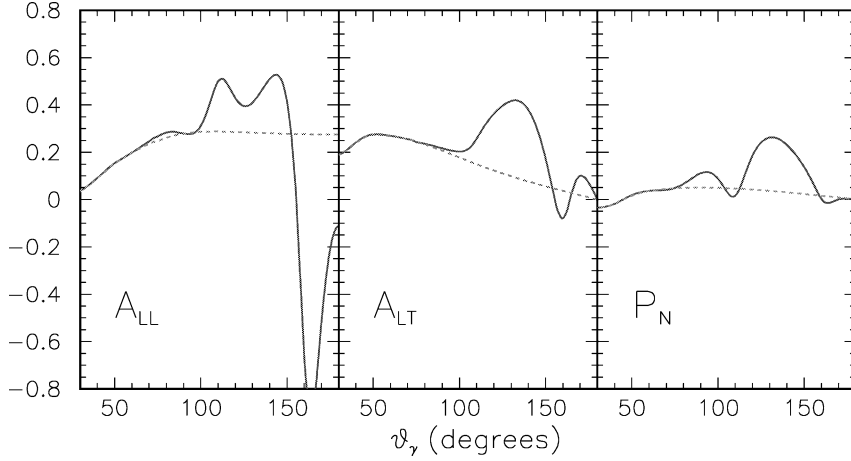


Fig. 2. Longitudinal (left), transverse polarization transfer (center) and induced polarization (right) in Compton scattering at $E_\gamma = 4$ GeV. Dashed lines are the contribution of Regge exchange in the t -channel. Solid lines are the final results, which include u -channel exchanges.

\hat{n} as [24]:

$$A \frac{d\sigma}{dt} = 2 \operatorname{Im}[W_{xy}(\hat{n}) - W_{yx}(\hat{n})], \quad (5)$$

where

$$W_{\mu\nu}(\hat{n}) = \sum_{m_1, m_2, m'_2} \langle m_1 | J_\nu^\dagger | m'_2 \rangle \times \langle m_2 | J_\mu | m_1 \rangle (\vec{\sigma} \cdot \hat{n})_{m'_2, m_2} \quad (6)$$

and J_μ is the current which couples to the initial photon. To have a non-vanishing polarization transfer we first need phases in the amplitudes which are provided by the Regge propagators. Second, a helicity flip in the proton sector is required. Neither the σ , f_2 nor two-gluon exchange amplitudes can flip the helicity of the proton. Only the π -exchange is able to provide this flip. The dominant contribution to A_{LL} for angles $\leq 120^\circ$ comes from the interference of the σ -exchange with the π -exchange. The interference of the other helicity conserving amplitudes (f_2 , two-gluons) with the π represents only a small correction. The contribution to P_N comes from the $\pi - \sigma$ interference, but it is proportional to the factor $(\frac{\vec{p} \times \vec{p}'}{(p^0 + m_N)(p'^0 + m_N)})$ which is small compared to the factors which takes part in the other asymmetries. Finally, for angles larger than $\approx 120^\circ$ the asymmetries are completely dominated by baryon exchanges in the u channel.

Deeply virtual Compton scattering

In a similar way, the DVCS amplitude can be deduced from the electroproduction amplitude of a (transverse) vector meson.

Let us first check the validity of the proposed model for meson electroproduction. The first difference with respect to the WACS case is that now we are interested in angular distributions at small angles or in the integrated cross section which is essentially given by the low $-t$ region. Moreover, for virtual photons one has to introduce electromagnetic form factors in the Regge-exchange amplitudes. The relevant amplitudes for HERMES energies and below are the σ , f_2 and two-gluon exchanges. The Q^2 dependence of the two-gluon and f_2 exchange contributions is built in the corresponding amplitudes [12]. Concerning the σ -exchange we have observed that a good description of $\sigma_{\gamma_T^* p \rightarrow p\rho}$ can be achieved with a monopole form factor $(1 + Q^2/\Lambda^2)^{-1}$ with $\Lambda^2 = 0.46 \text{ GeV}^2$ (this is in line with a VDM description of the $\gamma\rho\sigma$ coupling). In Fig. 3 we show the transverse, longitudinal and total cross sections for ρ -electroproduction at three different energies relevant for JLab and HERMES. We see that σ_T is very well reproduced in these cases, though σ_L is clearly overestimated. This is a longstanding problem in models of vector meson electroproduction and proposed solutions are based on a picture where the production of the meson takes place through open $q\bar{q}$ pairs [8,27]. Since our final

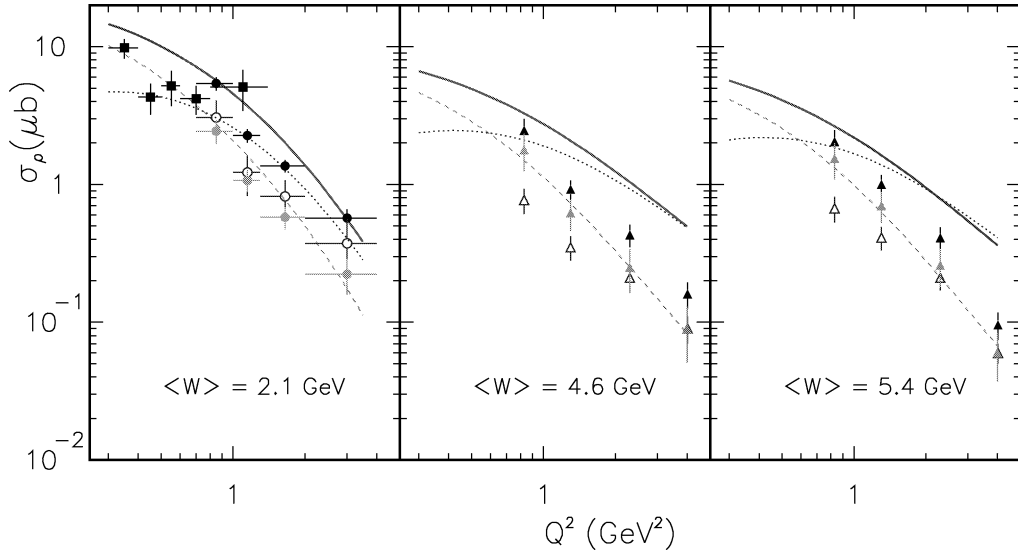


Fig. 3. Q^2 dependence of the longitudinal (dotted lines) and transverse (dashed lines) ρ production cross section for several values of W . Full lines: total cross section taking $\langle \epsilon \rangle = 0.95, 0.85, 0.72$ for $W = 2.1, 4.6, 5.4$ GeV, respectively. Experimental data from [25] (boxes) and [5] (circles) at $W = 2.1$ GeV and from [26] at the other energies. Black filled symbols: total, open symbols: longitudinal, faded symbols: transverse cross section.

goal is to apply the model to DVCS we do not address that problem here. The mean value $\langle \epsilon \rangle$ of the virtual photon polarization, corresponding to each experimental setting, has been used to compute the total cross section $\sigma_{\text{tot}} = \sigma_T + \langle \epsilon \rangle \sigma_L$.

The DVCS cross section is sensitive to the transverse amplitudes since the outgoing real photon has only transverse polarizations. The angular distributions for typical kinematics at JLab and HERMES are shown in Fig. 4. The VCS cross section is roughly five times smaller than predictions based on current modelisations of GPDs [28], and even for the region $\Phi = \pi$ where the Bethe–Heitler reaches its minimum, it overwhelms the VCS contribution.

Predictions for the measured beam asymmetries are also accordingly smaller than those based on GPDs, but in better agreement with experiments (Fig. 1). This observable is sensitive to the interference between VCS and Bethe–Heitler (BH) diagrams and is proportional to the imaginary part of the VCS amplitudes. The $\sin \Phi$ dependence of the asymmetry is a general feature of helicity conserving interactions for spin-1 particles. A Fourier decomposition of our results for A_{LU} gives $0.16 \sin(\Phi) + 0.008 \sin(2\Phi)$ for CLAS and

$-0.18 \sin(\Phi) - 0.028 \sin(2\Phi)$ for HERMES kinematics.

The agreement with the experimental data is remarkable also for the beam charge asymmetry (Fig. 5), that measures the real part of the amplitudes mentioned above. It has been argued in [30] that this observable is very sensitive to the D-term in the GPDs formalism. The D-term takes into account the scalar-isoscalar $q\bar{q}$ correlations in the proton. In our description, the σ -exchange seems to provide a good description of these correlations.

In the HERA energy range, the two gluon exchange mechanism dominates and leads to a rather good account of the H1 DVCS cross section [2] (1.5 nb, as compared to 4 ± 2 nb, at $Q^2 = 5 \text{ GeV}^2$), confirming the findings of [8].

4. Discussion

The good results obtained for the observables measured so far for DVCS, starting from the $\gamma_T^* p \rightarrow p\rho$ amplitudes, supports the conjecture that the hadronic component of the photon dominates at currently avail-

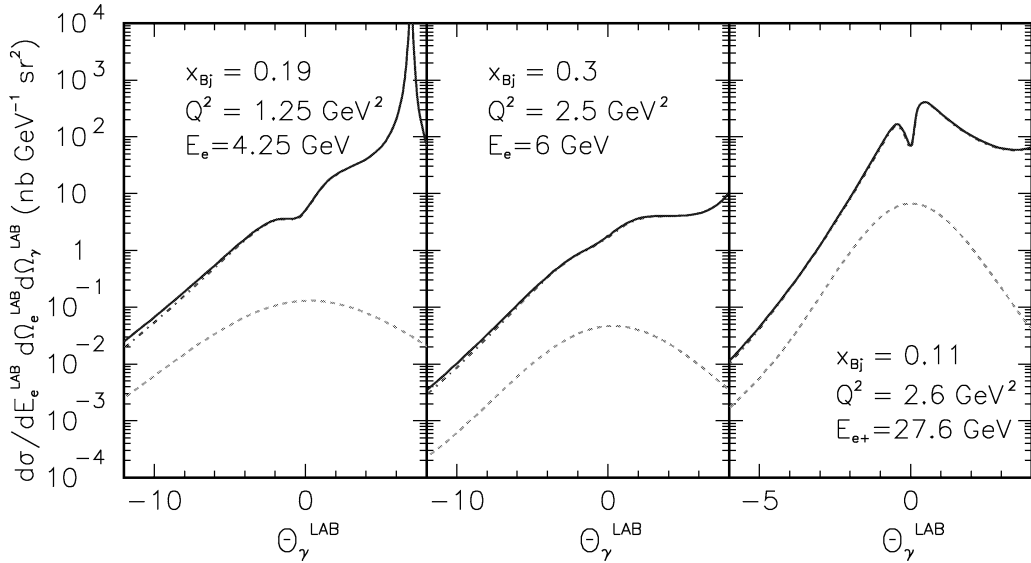


Fig. 4. Differential cross section for virtual Compton scattering for the kinematics relevant for JLab (left and center) and HERMES (right). Dashed-lines are the contribution of VCS and solid lines includes the Bethe–Heitler contribution.

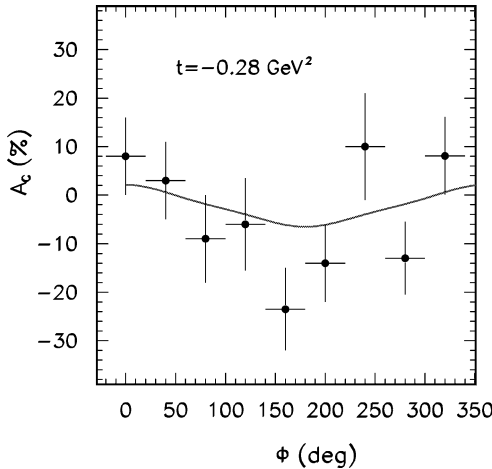


Fig. 5. Beam-charge asymmetry in DVCS for HERMES (preliminary data for [29]) with the same kinematics as in Fig. 1.

able energies. There is however a crucial difference between VCS amplitudes evaluated from GPDs, which show a $1/Q$ behavior (up to logarithmic corrections), and the ones used in our model, which have a steeper Q^2 dependence due to electromagnetic form factors. This means that at larger Q^2 the hadronic mechanism will fade out and that the pointlike coupling of the photon is expected to take over. The exact place where this happens is still under debate. Only exper-

iments will answer this question. For example, in a kinematics which will be reached at JLab when the beam energy is upgraded up to 12 GeV ($Q^2 = 8 \text{ GeV}^2$, $x_{Bj} = 0.55$) our model predicts an almost vanishing beam spin asymmetry (less than 2%), whereas models based on GPDs give results of the order of 30% at $t = -1 \text{ GeV}^2$ [31].

Another feature that could help to reveal the dominance of the hadronic component of the photon is the t -dependence of the weight s_1 of the leading term ($s_1 \sin \Phi$) in A_{LU} . Due to the phase of the Regge propagator, the sign of the imaginary part of the amplitudes changes and consequently the sign of A_{LU} (Fig. 6). This feature is sensitive to the energy s that controls the relative importance of different trajectories. An analysis of the t -dependence of A_{LU} at JLab energies would shed more light on the reaction mechanism.

In summary, the hadronic component of the outgoing photon saturates the cross section and reproduces spin observables which have been determined so far for real Compton scattering as well as deeply virtual Compton scattering. It should be emphasized that the ingredients of the model have been calibrated in meson photo- and electroproduction channels (ρ , ω , ϕ) and, therefore, predictions for WACS and DVCS involve no additional parameter or refitting of the existing ones. More experimental data are needed, both in

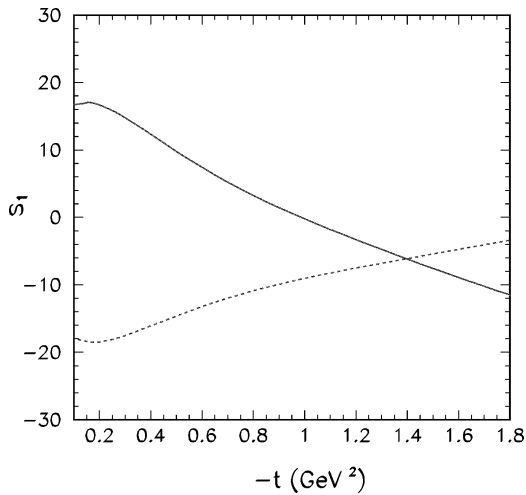


Fig. 6. Dependence of the leading term ($\sin \Phi$) with the momentum transfer for CLAS (solid line) and HERMES (dotted line). Kinematics as in Fig. 4 (left and right panel, respectively).

the vector meson production sector and in the Compton scattering sector, to map out in a comprehensive way the behavior of the hadronic component and find the best places to look for observables associated with the pointlike component of the photon in the initial as well as the final states.

Acknowledgements

We acknowledge F. Sabatié for help with Ref. [31]. This work is partially (F.C.) funded by European Commission IHP program (contract HPRN-CT-2000-00130).

References

- [1] K. Goeke, M.V. Polyakov, M. Vanderhaeghen, *Prog. Part. Nucl. Phys.* 47 (2001) 401.
- [2] C. Adloff, et al., H1 Collaboration, *Phys. Lett. B* 517 (2001) 47.
- [3] S. Stepanyan, et al., CLAS Collaboration, *Phys. Rev. Lett.* 87 (2001) 182002.
- [4] A. Airapetian, et al., HERMES Collaboration, *Phys. Rev. Lett.* 87 (2001) 182001.
- [5] D.G. Cassel, et al., *Phys. Rev. D* 24 (1981) 2787.
- [6] K. Ackerstaff, et al., HERMES Collaboration, *Phys. Rev. Lett.* 82 (1999) 3025.
- [7] F. Cano, J.-M. Laget, *Phys. Rev. D* 65 (2002) 074022.
- [8] A. Donnachie, J. Gravelis, G. Shaw, *Eur. Phys. J. C* 18 (2001) 539.
- [9] M. Battaglieri, et al., CLAS Collaboration, *Phys. Rev. Lett.* 87 (2001) 172002.
- [10] M.A. Shupe, et al., *Phys. Rev. D* 19 (1979) 1921.
- [11] M. Diehl, T. Gousset, B. Pire, J.P. Ralston, *Phys. Lett. B* 411 (1997) 193.
- [12] J.-M. Laget, *Phys. Lett. B* 489 (2000) 313.
- [13] B. Friman, M. Soyeur, *Nucl. Phys. A* 600 (1996) 477.
- [14] M. Guidal, J.-M. Laget, M. Vanderhaeghen, *Nucl. Phys. A* 627 (1997) 645.
- [15] D.E. Groom, et al., *Eur. Phys. J. C* 15 (2000) 1.
- [16] R. Machleidt, *Adv. Nucl. Phys.* 19 (1989) 189.
- [17] J.-M. Laget, in: P. Stoler, A. Radyushkin (Eds.), *Exclusive Processes at High Momentum Transfer*, Newport News, May 2002, World Scientific, Singapore, in press, hep-ph/0208213.
- [18] A.V. Radyushkin, *Phys. Rev. D* 58 (1998) 114008.
- [19] C. Bourrely, J. Soffer, E. Leader, *Phys. Rep.* 59 (1980) 95.
- [20] H.W. Huang, P. Kroll, T. Morii, *Eur. Phys. J. C* 23 (2002) 301.
- [21] M. Diehl, Th. Feldmann, R. Jakob, P. Kroll, *Phys. Lett. B* 460 (1999) 204.
- [22] M. Vanderhaeghen, P.A.M. Guichon, J. Vand de Wiele, *Nucl. Phys. A* 622 (1997) 144c.
- [23] A.M. Nathan, in: P. Stoler, A. Radyushkin (Eds.), *Exclusive Processes at High Momentum Transfer*, Newport News, May 2002, World Scientific, Singapore, in press.
- [24] J.-M. Laget, *Nucl. Phys. A* 579 (1994) 333.
- [25] P. Joos, et al., *Nucl. Phys. B* 113 (1976) 53.
- [26] A. Airapetian, et al., HERMES Collaboration, *Eur. Phys. J. C* 17 (2000) 389.
- [27] A.D. Martin, M.G. Ryskin, T. Teubner, *Phys. Rev. D* 55 (1997) 4329.
- [28] M. Vanderhaeghen, P.A.M. Guichon, M. Guidal, *Phys. Rev. D* 60 (1999) 094017.
- [29] F. Ellinghaus, in: *QCD Structure of the Nucleon, QCD-N'02*, Ferrara, 3–6 April 2002, *Nucl. Phys. A* 711 (2002) 171, hep-ex/0207029.
- [30] N. Kivel, M.V. Polyakov, M. Vanderhaeghen, *Phys. Rev. D* 63 (2001) 114014.
- [31] L. Mosse, Ph.D. Thesis, CEA-Saclay, 2002.